ACS Sustainable Chemistry & Engineering

Research Article

Cite This: ACS Sustainable Chem. Eng. 2019, 7, 10808−10820

pubs.acs.org/journal/ascecg

Preserving Both Lignin and Cellulose Chemical Structures: Flow-Through Acid Hydrotropic Fractionation at Atmospheric Pressure for Complete Wood Valorization

Zhaojiang Wang,[†,‡] Shi Qiu,[§] Kolby Hirth,[†] Jinlan Cheng,[†,∥] Jialong Wen,[⊥] Ning Li,[#] Yunming Fang,[§] Xuejun Pan,[#] and J.Y. Zhu*[,†,#]

[†]Forest Products Laboratory, USDA Forest Service, One Gifford Pinchot Drive, Madison, Wisconsin 53726, United States

[‡]State Key Laboratory of Biobased Material and Green Papermaking, Qilu University of Technology, Shandong Academy of Sciences, Jinan 250353, China

[§]National Energy R&D Research Center for Biorefinery, Department of Chemical Engineering, Beijing University of Chemical Technology, Beijing 100029, China

[∥]Jiangsu Co-Innovation Center of Efficient Processing and Utilization of Forest Resources, Nanjing Forestry University, Nanjing 210037, China

[⊥]Beijing Key Laboratory of Lignocellulosic Chemistry, Beijing Forestry University, Beijing, 100083, China

[#]Department of Biological Systems Engineering, University of Wisconsin-Madison, Madison, Wisconsin 53715, United States

Supporting Information

ABSTRACT: Poplar wood was rapidly fractionated via a flow-through reaction using aqueous solutions of an acid hydrotrope (AH), *p*-toluenesulfonic acid (*p*-TsOH), at temperatures below 98 °C. $^{13}C-^{1}H$ two-dimensional nuclear magnetic resonance (NMR) spectroscopic analyses demonstrated that the AH-solubilized lignins (AHLs) from a range of fractionation conditions with yields up to approximately 80% had a very high content of *β*-aryl-ether linkages compared to milled wood lignin (MWL) with a low enough condensation to facilitate subsequent reductive catalytic depolymerization resulting in a lignin monomer yield of over 30%. Gel-permeation chromatographic (GPC) and differential scanning calorimetric (DSC) analyses showed that the AHLs have high molecular weights and low glass transition temperatures T_g. These AHLs also have a pinkish color suitable for applications such as cosmetics and dye dispersants. AH fractionation (AHF) preserved the cellulose fraction as solid fibers also with a light pinkish color for the materials market and solubilized up to approximately 90% of xylan which can be converted to furfural using *p*-TsOH in the spent liquor without additional catalysts. The advantages herein are the use of one recyclable industrial chemical such as *p*-TsOH in an aqueous system below water boiling temperature to valorize all three major fractions of lignocelluloses in a short time frame, with very promising yields and well-preserved lignin and cellulose structure.

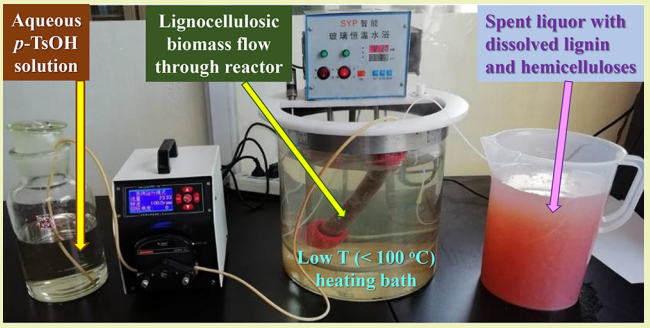

KEYWORDS: *Lignin valorization, Reduced lignin condensation, Acid hydrotropic fractionation (AHF), Catalysis/depolymerization, 2D NMR*

INTRODUCTION

Existing industrial and research practices of wood fractionation are focused on utilizing the cellulosic fraction, such as for producing papermaking fibers in the pulp and paper industry and cellulosic biofuels in the bioenergy arena, through delignification and prehydrolysis of hemicelluloses at elevated temperatures using harsh chemicals. Typical delignification processes in wood pulping take place at temperatures of 125−170 °C for a period of 2 h or more using sulfite or sodium hydroxide and sodium sulfide. Most promising fractionation or pretreatment processes for effective cellulosic biofuel production are operated between 120 and 200 °C.[1−5] The resultant lignins are chemically modified and highly condensed[6−9] with a low content of *β*-O-4 aryl-ether linkages and therefore are difficult to valorize.[9−11] Chemical structures of these technical lignins are well characterized and compared in the literature.[9,11] Combustion of lignin from wood pulping, a low-value utilization, is commonly practiced in pulp mills because it achieves pulping chemical recovery and contributes to mill energy self-sufficiency, which is critical to sustainable

Received: March 22, 2019
Revised: April 22, 2019
Published: May 16, 2019

DOI: 10.1021/acssuschemeng.9b01634
ACS Sustainable Chem. Eng. 2019, 7, 10808−10820

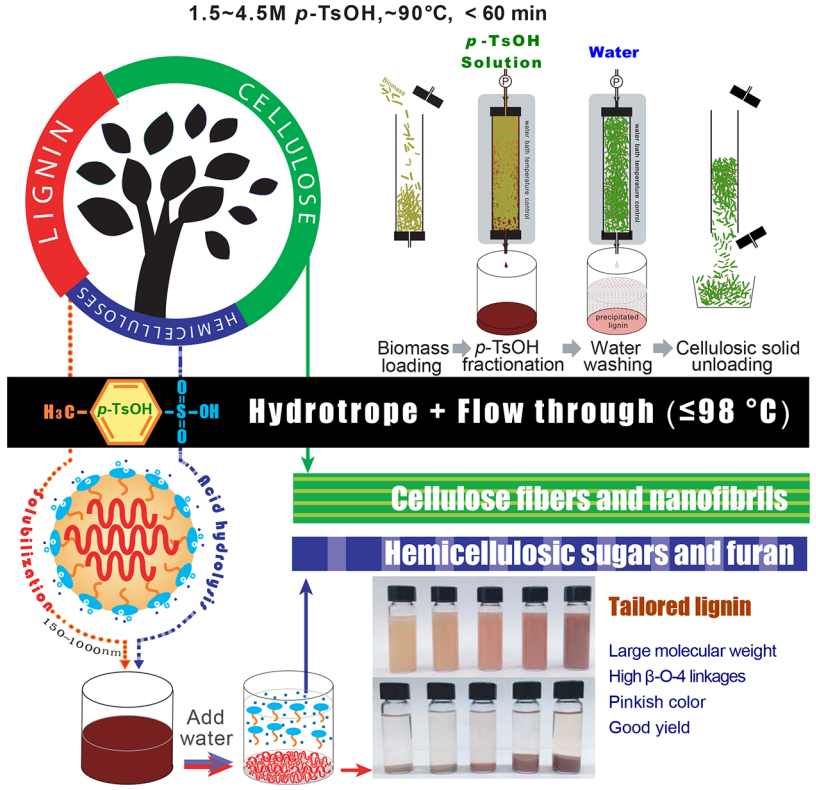

Figure 1. Description of soft fractionation of wood using acid hydrotrope *p*-TsOH in a flow-through reactor configuration into a cellulosic fiber fraction and a liquor fraction that contains dissolved lignin and hemicellulosic sugars.

and economical pulp mill operation. However, lignin valorization other than for boiler fuel is a key to a sustainable and economical operation of future biorefinery.

To avoid lignin condensation, reductive catalytic lignin fractionation (RCF)[12,13] was applied recently to produce lignin monomers or aromatics directly from lignocelluloses via one-step depolymerization.[9,14] However, this approach often uses organic solvents to improve lignin yield or is carried out at temperatures over 170 °C, equivalent to or higher than temperatures employed in existing fractionation/pretreatment or industrial pulping processes.[14] Valorization of the carbohydrate fraction, approximately 65% of lignocellulosic biomass, remains unaddressed,[13,15−17] though limited efforts have been made.[18−20] Issues associated with recycling of catalysts that remain mixed with the carbohydrate fraction also need to be fully resolved.[12,13,21]

The conventional two-step approach, i.e., fractionation first, such as wood pulping, followed by lignin conversion, can be an attractive pathway if the fractionated lignin is not substantially condensed with sufficiently high content of β-O-4 ether linkages. A variety of catalytic routes can produce high-yield, low-molecular-weight lignin aromatics provided that the fractionated lignin is not condensed.[14,22] Furthermore, the fractionated uncondensed lignin polymers with high molecular weight are highly attractive for direct utilization, i.e., without further depolymerization, in composites.

Here we propose the concept of soft fractionation to preserve key properties of lignin and cellulose for complete valorization of lignocelluloses for a wide product portfolio. As opposed to carbohydrate-solvent systems that hydrolyze carbohydrates to sugars in order to obtain uncondensed solid lignin,[23] the soft fractionation concept takes advantages of cellulose as a polymer molecule that is highly organized and recalcitrant to depolymerization and useful in materials applications, such as textile fibers[24−26] and cellulose nanomaterials,[27,28] while preventing substantial lignin condensation in delignification. It deviates from traditional wood pulping and sugar-centric processes that usually result in substantially condensed lignin. It also differs from the few elegant catalytic-centric studies,[21,29−32] which use expensive first-step fractionation, such as organic solvents at high loadings, and are often carried out at high temperatures or even supercritical conditions to fractionate lignin suitable for producing low-molecular-weight aromatics. To demonstrate the soft fractionation concept, here we use *p*-toluenesulfonic acid (*p*-TsOH), a relatively inexpensive industrial chemical, as a hydrotrope for low-temperature (≤98 °C) and therefore at atmospheric pressure but with selective fractionation of poplar wood[33] at high yield in a flow-through configuration as shown in Figure 1. After solids and liquor separation through filtration, the dissolved lignin was separated simply by diluting the spent liquor using water to below the *p*-TsOH minimal hydrotrope concentration (MHC).[33] The dissolved hemicellulosic sugars can be dehydrated into furfural using *p*-TsOH in the spent liquor after reconcentrating the lignin-separated weak spent liquor, without additional acid,[28] facilitating the recovery and reuse of the *p*-TsOH.

Using a flow-through reaction to obtain time-dependent data and two-dimensional (2D) $^{1}H-^{13}C$ nuclear magnetic resonance (NMR) and gel-permeation chromatographic (GPC) analyses, this investigation is focused on the lignin chemical structure and lignin condensation conditions and mechanism, which differentiates from our initial concept demonstration study using a batch reaction that is focused

DOI: 10.1021/acssuschemeng.9b01634
ACS Sustainable Chem. Eng. 2019, 7, 10808−10820

on lignin dissolution.[33] Specifically, this study validated the hypothesis proposed in the initial study: i.e., through proper process control, an acid-hydrotrope-dissolved lignin (AHL) with well-preserved chemical structure and high content of β-O-4 ether linkages at high yield can be obtained. The study also demonstrated high yields of lignin monomers and low-molecular-weight aromatics from this type of AHL through reductive catalytic depolymerization. This acid hydrotropic fractionation (AHF) below the boiling point of water under atmospheric pressure, using only one chemical, is advantageous in addressing capital and operating cost issues. It also can alleviate market mismatch by producing both high-quality cellulose and lignin fractions suitable for developing a variety of bioproducts with growing markets.

MATERIALS AND METHODS

Materials. Logs of poplar NE222 (*Populus deltoides* Bartr. ex Marsh. × P. *nigra* L.) were harvested from Hugo Sauer Nursery in Rhinelander, Wisconsin, USA, by Dr. R. Zalesny Jr., Northern Research Station, USDA Forest Service. Logs were debarked manually and chipped at the Forest Products Laboratory, USDA Forest Service, Madison, Wisconsin. The wood chips were then ground into 20-mesh particles using a Wiley mill (model no. 2, Arthur H. Thomas Co.) for fractionation. Kraft lignin (lignin, alkali) and *p*-TsOH monohydrate were purchased from Sigma-Aldrich (Missouri, USA).

Wood Fractionation Using Aqueous *p*-TsOH Solution. The flow-through reaction system consisted of a reservoir containing fresh aqueous *p*-TsOH solution, a peristaltic pump, a polypropylene column (100 mm length ×8 mm diameter) submerged in a temperature-controlled water (or oil depending on temperature) bath, a spent liquor collection container in an ice water bath, and a connecting silicon tubing. A nylon mesh screen (60−120 US standard mesh, sieve size from 0.125 to 0.25 mm) was used at the outlet of the column. Some scale-up runs were carried out using a 150 mL column (300 mm length × 25 mm diameter, Figure S1) using a stainless steel screen of 80 mesh (0.18 mm) to obtain enough material for full characterization. Flow-through fractionation consists of four steps (Figure 1): biomass loading, *p*-TsOH fractionation, water washing, and solid residue unloading. All flow-through fractionation runs were conducted below 100 °C at atmospheric pressure (see Table S1 for detailed conditions). A total of 1.3 g of oven dry (OD) weight Wiley-milled poplar wood was placed in the column and heated to the desired fractionation temperature. Fresh *p*-TsOH solution of the desired concentration at the fractionation temperature was then rapidly pumped through the biomass at 4.15 mL/min to fill the void space within 1 min. The flow rate was then reduced to 0.3−1.3 mL/min, depending on the preset reaction time, with a final liquor-to-wood ratio of 20:1 (mL/g). The residence time of the liquor through the column was calculated (Table S1). The spent liquor was collected. After the fractionation step, approximately 60 mL of deionized water was flowed through the column to wash out residual *p*-TsOH spent liquor as indicated by the pH of the washing filtrate (Table S2). The washed water-insoluble solids (WIS) residue was then taken out of the column and stored for further analysis. Solid yield was determined gravimetrically.

For comparison purposes, batch fractionation runs were also conducted (Table S1) using 1.3 g of biomass (OD) with 26 mL of *p*-TsOH solution in a 50 mL flask placed in a temperature-controlled water or oil bath and stirred by a magnetic bar at 120 rpm. After the fractionation, solids and spent liquor were separated through filtration. The solids were washed using 60 °C deionized water to result in a colorless filtrate of approximately pH 6.5.

Spent Liquor Aging Experiments. To investigate AHL repolymerization (or condensation) in the spent liquor, a collected spent liquor was stored at room temperature or maintained at the fractionation temperature for a period of time. Aging studies (Table S3) lasted 24−72 h at room temperature, and 15−30 min at the fractionation temperature.

AHL Isolation and Purification. To reduce AHL condensation, the collected spent liquor was immediately transferred to a 250 mL flask, combined with washing filtrates, and then diluted with water to below the *p*-TsOH MHC of 0.67 mol/L[33] to precipitate AHL. After the supernatant was siphoned off, the remaining precipitated wet solids were transferred to a centrifuge tube and further diluted with water, mixed, then centrifuged for 10 min at 10 000 rpm. The supernatant was decanted and discarded. This process was repeated at least five times to remove *p*-TsOH and other soluble products from fractionation. Preferably, the spent liquor should be collected immediately after flowing out of the reactor into a 250 mL flask containing cold water to chill (Mode D in Figure S1). After the supernatant was siphoned off from the combined diluted spent liquor, the wet AHL solids can go through dialysis for better removal of *p*-TsOH. The purified AHL was lyophilized at −55 °C prior to GPC or NMR analyses.

Time-Dependent Delignification and AHL Color. AHL UV−vis absorption coefficients were determined experimentally. Two milligrams of the purified AHL was dissolved in 0.3 mol/L NaOH solution with stirring for 1 min. The AHL solution was then diluted 20 times using 0.02 mol/L NaOH to result in AHL concentration of approximately 13 mg/L for UV−vis absorption measurements (model 845, Agilent Technologies, Palo Alto, California). NaOH solution of 0.02 mol/L was used as a blank. Extinction coefficients at 280 and 410 nm were calculated according to the Beer−Lambert law. For comparison purposes, UV−vis spectra of a commercial kraft lignin were also obtained in the same way.

To quantify time-dependent delignification during fractionation, 100 μL aliquots of liquor samples were taken periodically from the exit of the flow-through reactor and transferred to a centrifuge tube to separate and purify AHL, as described above. AHL concentration in a liquor sampled at a given fractionation time was determined through UV−vis measurements at 280 nm. The extinction coefficient of AHL was calibrated from purified AHL samples obtained from the same fractionation condition as described above (Figure S2).

AHL color was measured by a hand-held color reflectance spectrometer (X-Rite SP64, Grand Rapids, Michigan, USA). Purified AHL was spread on a piece of white paper for direct spectrophotometric measurements. CIE (International Commission on Illumination) values $L^*a^*b^*$ were directly obtained from X-rite SP64. Adobe illustrator was used to reproduce the color in a color pad for comparison with the corresponding AHL image.

Chemical Compositional Analyses. Chemical compositions of untreated poplar wood and *p*-TsOH fractionated poplar WISs were analyzed by the Analytical Chemistry and Microscopy Laboratory at the USDA Forest Service, Forest Products Laboratory (Madison, WI, USA). Briefly, woody solids were first oven-dried overnight at 105 °C, cooled, then Wiley-milled to 20-mesh powder. Carbohydrates in the powders were solubilized using the conventional two-step sulfuric acid hydrolysis procedure as described previously[34] and then analyzed using ion chromatography (ICS-5000, Dionex, Thermo Scientific) with amperometric detection (HPAEC-PAD). Lignin was determined gravimetrically.

Molecular Weight Determination by Gel-Permeation Chromatography (GPC). Separated AHL was air-dried and then acetylated by adding 0.2 mL of pyridine-acetic anhydride solution (1:1) and then sealed and stored in the dark for 72 h at room temperature. After the pyridine-acetic anhydride was removed by a stream of air, the acetylated lignin was dissolved in 1.0 mL of tetrahydrofuran (THF) and then analyzed for molecular weight distribution using GPC on a high-performance liquid chromatograph (LC) system (ICS-3000, Dionex, Thermo Scientific, Sunyvale, CA) as described previously.[23,33] The GPC system was equipped with three 300 × 7.8 mm Phenogel 5U columns (10 000, 500, and 50 Å) and a 50 × 7.8 mm i.d. Phenogel 5U guard columns (Phenomenex, Torrance, CA), and a variable wavelength UV detector at 280 and 254 nm for detecting lignin with polystyrene as standards. The GPC was operated at 30 °C using THF as eluent at a flow rate of 1 mL/min.

AHL Structure Analyses by NMR. $^{13}C-^{1}H$ NMR analysis of AHL was performed using a Bruker 500 MHz Avance III HD

DOI: 10.1021/acssuschemeng.9b01634
ACS Sustainable Chem. Eng. 2019, 7, 10808−10820

Table 1. Chemical Compositions of Aqueous *p*-TsOH Fractionated Poplar Wood Samples in a Flow-Through Reactor under a Range of Conditions[a]

	WIS					spent liquor		
sample label	solid yield (%)	glucan (%)	xylan (%)	mannan (%)	lignin (%)	xylose (%)[b]	acetic acid (%)[c]	furfural (%)[d]
untreated poplar	100	45.7	14.6	4.6	23.8			
P1.5T70t30	90.1	45.9 (90.6)	12.6 (76.3)	2.3 (45.1)	22.0 (83.3)		2.3	no
P1.5T80t30	86.1	47.9 (90.1)	10.2 (58.7)	2.4 (44.7)	21.6 (77.9)			no
P1.5T80t60	71.2	57.6 (89.8)	6.1 (29.2)	2.9 (45.2)	19.5 (58.4)			no
P1.5T80t90	72.3	56.2 (88.9)	6.4 (31.1)	2.3 (36.2)	19.8 (60.3)		3.1	no
P2.5T70t30	85.9	47.8 (89.8)	9.5 (54.4)	2.4 (45.5)	21.7 (78.4)		2.8	no
P2.5T75t20	79.9	52.9 (92.5)	8.5 (45.5)	2.6 (45.2)	19.9 (66.9)			no
P2.5T80t60	64.8	64.4 (91.3)	6.3 (27.3)	2.0 (27.4)	15.1 (41.1)	63.2	3.5	no
P2.5T85t60	60.3	70.2 (92.7)	4.4 (17.7)	3.0 (39.1)	12.2 (30.9)	71.9	3.8	no
P2.5T90t60	55.7	76.8 (93.5)	4.9 (18.3)	2.1 (25.1)	8.8 (20.7)	77.7	4.0	no
P2.5T98t40	54.0	81.4 (96.2)	3.0 (11.1)	2.4 (22.0)	8.0 (18.1)	80.7	4.0	no
P3.5T80t40	58.6	70.6 (90.5)	5.7 (22.5)	2.7 (33.9)	10.1 (24.9)		3.8	no
P3.5T80t60	58.6	70.0 (89.7)	5.2 (20.3)	3.1 (39.5)	9.5 (23.4)			no
P4.5T70t30	67.0	62.1 (91.0)	7.0 (31.3)	2.8 (40.2)	16.1 (45.2)	66.7	3.7	no
P2.5T90t60bat	52.1	72.6 (82.7)	2.4 (8.3)	2.8 (32.1)	9.9 (21.7)	74.7	4.1	3.0

[a]The numbers in the parentheses are the percentage retained in WISs based on the untreated wood. [b]Contains xylose monomers and oligomers, expressed as the xylan equivalent of untreated biomass. [c]Expressed as mass percentage of untreated biomass. [d]Expressed as the pentosan equivalent of untreated biomass.

spectrometer equipped with a Prodigy (liquid N_2-cooled) 5 mm gradient TCI (inverse configuration) $^{1}H/^{13}C/^{15}N$ cryo-probe. Approximately 60 mg of purified AHL was dissolved in 0.6 mL of DMSO-d_6, referenced at 39.5/2.5 ppm. The $^{13}C-^{1}H$ heterogeneous single quantum correlation (HSQC) experiment was performed using the Bruker standard pulse program hsqcetgpsisp 2.2 (gradient-edited, sensitivity enhanced 2D-HSQC using adiabatic pulses for inversion and refocusing) with nonuniform sampling of 50%. Spectra were acquired using 40 scans and an interscan delay (D1) of 1 s for a total acquisition time of 3 h with a 12 ppm sweep width in F2 (^{1}H) using 1024 data points for an acquisition time (AQ) of 85 ms; and in F1 (^{13}C), a 215 ppm sweep width using 512 increments for AQ of 9.74 ms. Data processing used squared cosine-bell in F1 and F2, resulting in a 1024 × 1024 data matrix. Topspin 3.7p17 was used for interactive integration of 2D crosspeaks. Graphical figures were prepared using Adobe Illustrator from spectra exported from MestReNova/TopSpin in the pdf format.

Quantitative ^{31}P NMR was employed to measure the contents of hydroxyl and carboxyl groups in AHL.[35] Before determination, 20 mg of purified AHL was dissolved in 500 μL of pyridine-d_5/$CDCl_3$ solvents (1.6:1, v/v) with stirring, followed by the addition of 100 μL of cyclohexanol (10.85 mg/mL in pyridine-d_5/$CDCl_3$ solvents) as an internal standard and 100 μL of chromium(III) acetylacetonate solution (5 mg/mL in pyridine-d_5/$CDCl_3$ solvents) as relaxation reagent. This mixture was reacted with 100 μL of phosphitylating reagent (2-chloro-4,4,5,5-tetramethyl-1,3,2-dioxaphospholane, TMDP) for about 10 min and then transferred to a 5 mm NMR tube for subsequent NMR analysis. Each ^{31}P NMR acquisition was performed with a 25-s delay between 90° pulses. An inverse gated decoupling pulse sequence was used to obtain quantitative spectra. A minimum of 150−200 transients was acquired for each sample. The acquisitions were performed at room temperature using a 62-ppm sweep width (TD = 32,768) and a 4-Hz line broadening. Chemical shifts were calibrated relative to the cyclohexanol as an internal standard peak at δ_C = 145.1 ppm.

AHL Depolymerization Using Ru/C. Depolymerization reactions of 0.1 g of AHL or MWL, or raw poplar with 0.15 g of Ru/C, 20 mL of methanol were carried out in a 50 mL high-pressure autoclave.[12] The reactor was first purged with nitrogen to remove air and then pressurized to 1 MPa and heated to 250 °C for 3 h with stirring. At the end of the reaction, the reactor was cooled to room temperature in an ice bath. The resulting mixture was separated by filtration to obtain lignin oil. Methanol was removed by evaporation. When using raw poplar, the poplar wood powder was dried in an oven overnight. The lignin oil from the raw poplar was further extracted by dichloromethane to determine delignification based on the poplar Klason lignin content of 23.8 wt %. The bio-oil yield was calculated based on the initial lignin or biomass intake on a mass basis using the following equation.

$$\text{bio-oil yield (\%)} = \frac{\text{mass of bio-oil}}{\text{initial mass of feedstock (lignin or biomass)}} \times 100 \quad (1)$$

Lignin oil samples were dissolved in THF solution at 2 mg/mL and filtered with a 0.2 μm PTFE membrane before analyses for molecular weight using GPC through UV detection at 254 nm. The GPC system was equipped with an HPLC (1525, Agilent technologies, Palo Alto, CA, USA) and two columns (Waters Styragel HR 4E THF and Waters Styragel HR 5E THF column). The column was heated at 35 °C. THF was used as eluent at 1 mL/min. Commercial polystyrene standards were used as a standard for molecular weight calibration.

Lignin oils were further analyzed using a GC-MS system (7890A/5975C, Agilent Technologies, Palo Alto, CA, USA) equipped with a HP-5 column (30 m × 0.25 mm). The column was heated to 50 °C and held for 1 min and then heated up to 300 °C at 5 °C/min and held for 4 min. The analyses of the mass spectra were mainly based on an automatic library search of Agilent NIST database (version 2.0). The identification and quantification of phenolic monomers in bio-oils were obtained using standard samples from a commercial source or independent synthesis. Standard curves were prepared for each monomer compound as demonstrated previously.[36]

RESULTS AND DISCUSSION

Mass Balance Analyses of Soft Fractionation Using Aqueous *p*-TsOH. Chemical compositions of the fractionated washed water-insoluble solids (WIS) and components retained on WIS, as well as the composition of the collected spent liquors from different fractionation conditions, are listed in Table 1. Flow-through fractionation using aqueous *p*-TsOH solution dissolved 79.3% lignin at 90 °C in 60 min using 2.5 mol/L *p*-TsOH (P2.5T90t60). Approximately 82.3% xylan was dissolved, while 93.5% glucan was preserved in the WIS under this condition. Interestingly, 77.7% of the xylan can be recovered from the collected spent liquor in the form of xylose

DOI: 10.1021/acssuschemeng.9b01634
ACS Sustainable Chem. Eng. 2019, 7, 10808−10820

and xylooligomers (Table 1, Figure S3), both of which can be easily dehydrated into furfural (a valuable chemical) with good yield using the *p*-TsOH as catalyst in the spent liquor.[28] Compared with batch fractionation under the same set of conditions, the flow-through reaction preserved more carbohydrates such as glucan and xylan (Table 1).

Increasing *p*-TsOH concentration improved dissolution of lignin and hemicelluloses (xylan and mannan), as shown in Table 1. Glucan retention in WISs remained at approximately 90% for the range of *p*-TsOH concentrations used, suggesting an excellent selectivity in solubilizing lignin and hemicelluloses while preserving cellulose using aqueous *p*-TsOH. The results in Table 1 also show that increasing reaction temperature improved the dissolution of lignin and hemicelluloses. At low *p*-TsOH concentrations of 1.5 mol/L, increasing the reaction time from 30 to 60 min substantially improved lignin and xylan dissolution but did not result in increasing cellulose degradation (comparing P1.5T80t30 with P1.5T80t60), and further increasing to 90 min resulted in negligible effects. At *p*-TsOH concentration of 2.5 mol/L with a 60 min flow-through reaction, lignin dissolution was increased from approximately 59% to approximately 79% when the temperature was raised from 80 to 90 °C. Further increasing temperature to 98 °C showed a minor effect on lignin solubilization but increased xylan dissolution to approximately 89% from 82% (compare P2.5T90t60 with P2.5T98t40). This good selectivity in preserving cellulose while solubilizing lignin and xylan can be visualized by plotting the results in Table 1 (Figure S4). Xylan recovery was compared to the GVL process[37] (Figure S3).

Time-Dependent Study of Aqueous *p*-TsOH Fractionation. The time-dependent concentrations of dissolved lignin, xylose, and acetic acid in spent liquor were obtained by periodic sampling of the spent liquor. Figure 2 shows results from three fractionations at different severities. The time-dependent concentration profiles indicate that acetic acid reached a peak value earlier than xylose, suggesting that deacetylation was faster than acid hydrolysis of xylan, especially at the early stage of reaction (Figure S5). This is consistent with the premise that deacetylation on xylan backbone facilitates xylan dissolution.[38] The results in Figure 2 also indicate that lignin dissolution was rapid and took place at the very early stage of fractionation, especially at the highest *p*-TsOH concentration. As a result, the *p*-TsOH liquor-to-wood ratio can be reduced by half by reducing the flow-through time (by half) without a noticeable effect on lignin dissolution (yield). It appears that the concentration of dissolved AHL peaked even earlier than acetic acid, suggesting that bulk lignin not chemically bonded with xylan was more quickly solubilized through the aggregation process by hydrotrope *p*-TsOH. Increasing fractionation severity not only improved lignin and xylan dissolution but also accelerated dissolution, as shown by the left shift of the peaks of the dissolved xylan, AHL, and acetic acid profiles (Figure 2A–C).

AHL Optical Properties. The conventional technical lignin from kraft pulping is dark brown in color[39] partly due to chemical condensation, which prevents its use in applications sensitive to colors, such as cosmetics and dispersants for dyes. AHLs and their corresponding cellulosic fractions have a pinkish tint (Figure S2). The reproduced color from the measured CIE (International Commission on Illumination) *L*a*b** values of AHL samples was compared with the corresponding AHL image (Figure 3). Increasing acid concentration and fractionation temperature resulted in a

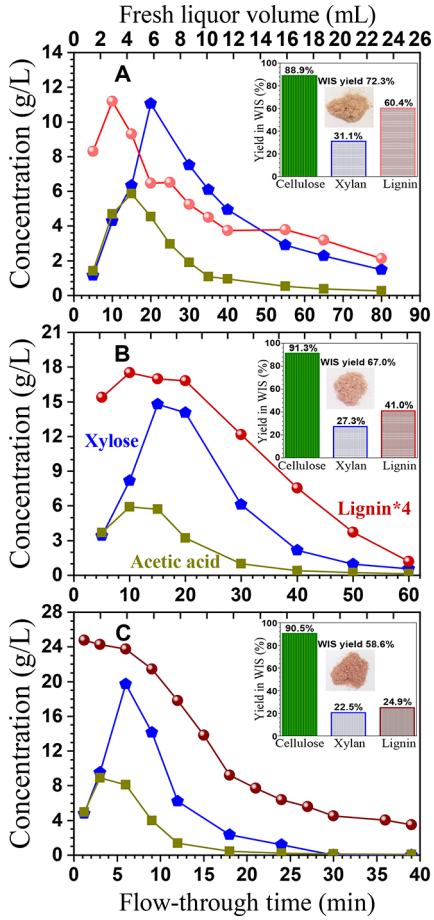

Figure 2. Time-dependent concentration profiles of xylose, acetic acid, and lignin in the process liquor. (A) P1.5T80t90; (B) P2.5T80t60; (C) P3.5T80t40.

darkening color; therefore, there is a trade-off between AHL yield (the amount of lignin dissolution) and lignin color. However, a pink AHL was obtained even at P2.5T98t40 with a respectable AHL yield of over 80% (Figure 3).

Aging spent liquor also resulted in a darkening color of AHLs (Figure 3, Figure S6) due to the extended contact time between the AHL and *p*-TsOH for repolymerization (condensation) reactions to take place. Batch fractionation had the same effect as spent liquor aging because most lignin was dissolved rapidly in the early stage of reaction (Figure 2) and vulnerable to repolymerization with extended time.

To investigate the formation of chromophore groups, we used model lignin guaiacylglycerol-*β*-guaiacyl ether (GG) during acidolysis in 2.5 M *p*-TsOH at 90 °C (description for Figure S7) and identified reaction product 1-hydroxy-3-(4-hydroxy-3-methoxyphenyl)-2-propanone (HHMP) from cleavage of *β*-O-4 ether bonds. HHMP is one of the Hibbert's ketones (HK) from depolymerization[22,23] that were identified from our 2D NMR spectra at *δ*C/*δ*H 67.1/4.19 (Figure 4). We also verified the formation of coniferyl aldehyde from further dehydration of HHMP.[29] The conjugated double bond and aldehyde auxochrome group in coniferyl aldehyde and the ketone auxochrome group in HHMP contribute to the pinkish color observed derived from dehydrogenative polymerization resulting in extended conjugation.[40] Under harsh conditions, the darker brown color results from condensation reactions (Figure S7).

DOI: 10.1021/acssuschemeng.9b01634
ACS Sustainable Chem. Eng. 2019, 7, 10808–10820

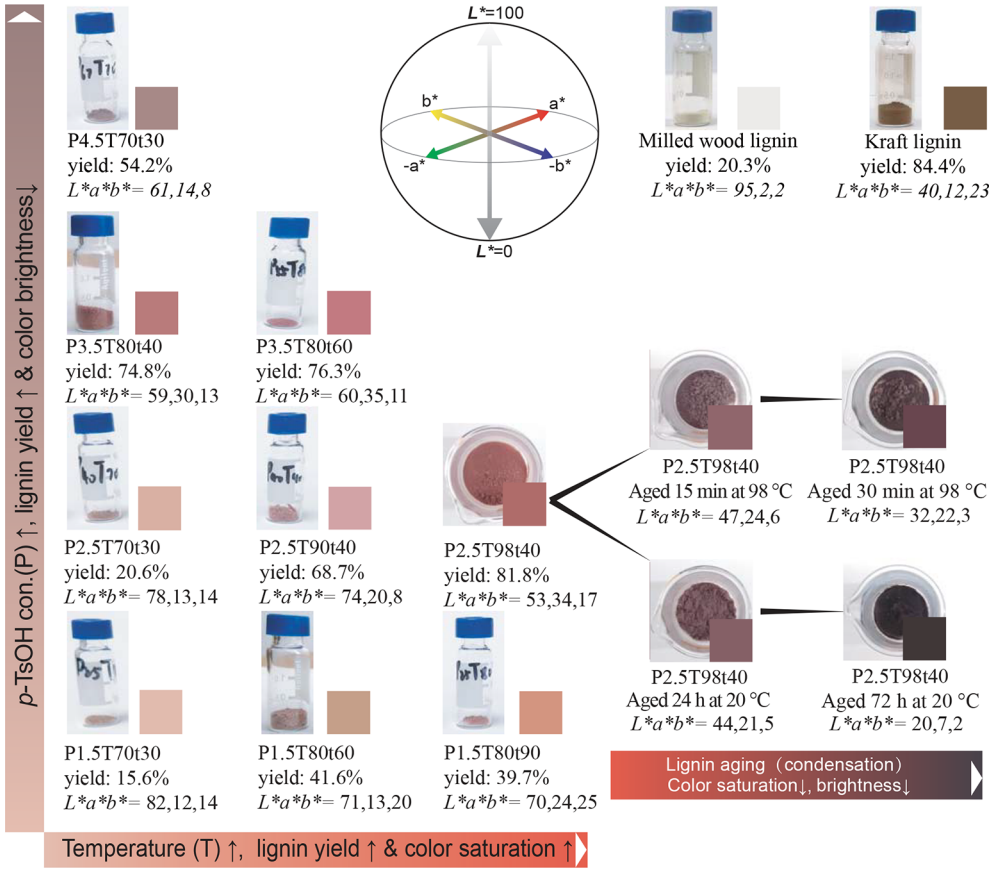

Figure 3. Effects of *p*-TsOH concentration and fractionation temperature on the color of the resultant AHLs in comparison with the color of MWL and KL. The colors of the square pads were constructed based on the measured CIE *L*a*b**.

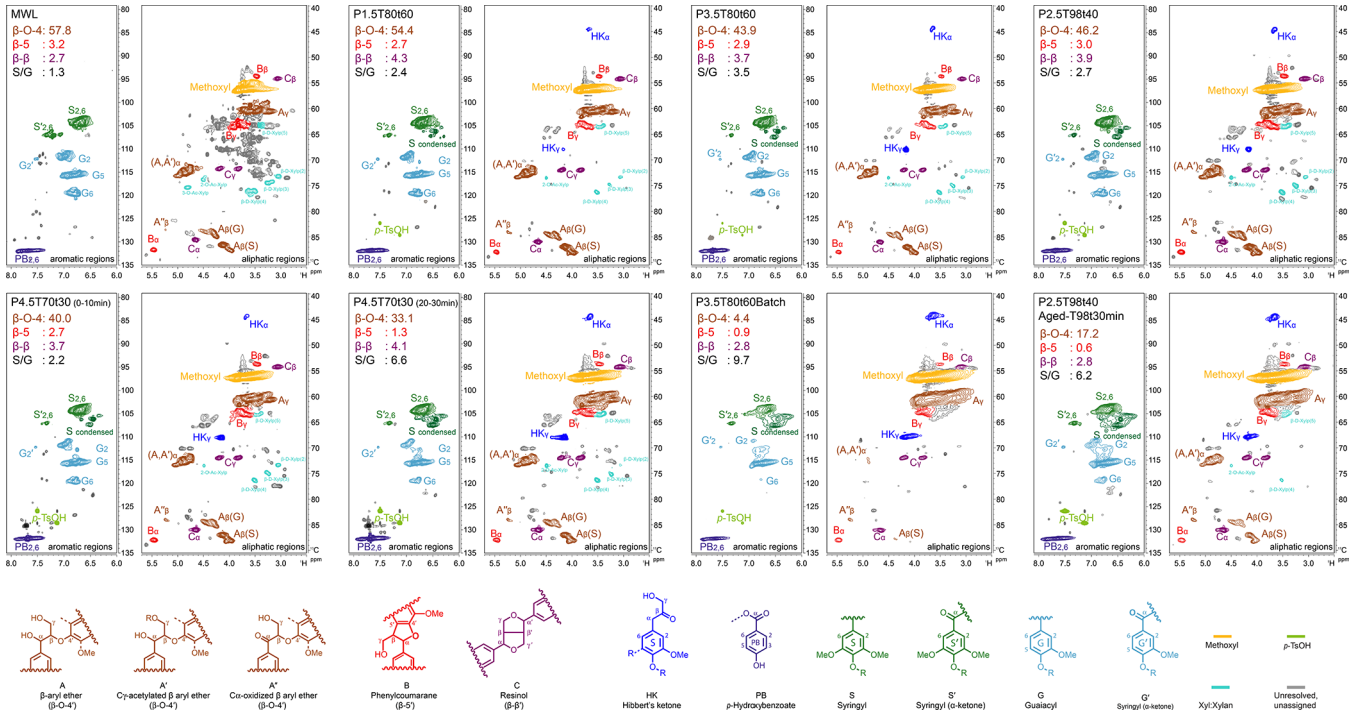

Figure 4. 2D $^{1}H-^{13}C$ NMR identified main classical and acylated substructures involving different side-chain linkages and aromatic units of MWL and AHLs from various *p*-TsOH fractionation conditions. HK_Y stands for Hibbert's ketones in the *γ*-position.

AHL Chemical Structures by NMR Spectroscopy. 2D $^{1}H-^{13}C$ NMR analyses can provide important lignin chemical structural information. The side chains (δ_C/δ_H 50−90/2.5−6.0 ppm) and the aromatic (δ_C/δ_H 80−135/6.0−8.0 ppm) regions

DOI: 10.1021/acssuschemeng.9b01634
ACS Sustainable Chem. Eng. 2019, 7, 10808−10820

Table 2. Quantifications of Side Chains and Aromatic Units Present in Lignin from $^{13}C-^{1}H$ 2D NMR HSQC Spectra

	sample labels	β-O-4[a]	β-5[a]	$\beta-\beta$[a]	HK	*p*-hydroxy benzoate (PB)[a]	S[b]	$S_{condensed}$	G[b]	H[b]	S/G
extraction	MWL	57.8	3.2	2.7		21.9	56.8		43.2		1.3
flow-through	P1.5T80t60	54.4	2.7	4.3	0.06	26.2	70.7	1.8	29.3		2.4
	P2.5T80t60	47.6	2.5	4.5	1.1	34.8	75.8	5.0	24.2		3.1
	P3.5T80t60	43.9	2.9	3.7	1.7	36.6	77.6	7.8	22.4		3.5
	P2.5T70t30	52.4	2.8	3.8	0.4	38.4	72.2	4.3	27.8		2.6
	P2.5T90t60	36.1	2.5	4.3	4.5	40.0	77.8	10.6	22.2		3.5
	P4.5T70t30	37.6	2.2	3.9	2.9	80.1	79.4	9.5	20.6		4.6
flow-through P2.5T98t40 − aging@	P2.5T98t40	46.2	3.0	3.9	1.9	28.7	72.6	7.2	27.3		2.7
	−T20t24h	32.1	1.0	4.4	3.4	42.5	85.6	9.0	14.4		5.9
	−T20t72h	21.7	0.6	2.7	7.2	62.2	87.6	22.2	12.4		7.1
	−T98t15 min	28.9	2.1	4.1	5.4	28.6	80.6	15.3	19.4		4.1
	−T98t30 min	17.2	0.6	2.8	6.9	25.3	86.2	24.1	13.8		6.2
time-dependent P4.5T70t30	0−10 min	40.0	2.7	3.7	1.6	53.4	68.3	7.7	31.7		2.2
	10−20 min	39.6	1.6	3.8	2.0	73.0	83.2	8.4	16.8		5.0
	20−30 min	33.1	1.3	4.1	5.5	114.0	86.8	12.4	13.2		6.6
batch	P2.5T90t60	10.0	1.2	3.1	9.9	21.4	87.9	30.9	12.1		7.3
	P3.5T80t60	4.4	0.9	2.8	12.6	17.0	90.7	40.7	9.3		9.7
literature data of technical and organosolv lignin[c]	Alkali Kraft	5.2	0	0.9		0	0		97	3	0
	indulin Kraft	6.1	0.3	1		0	0		97	3	0
	Soda P1000	3.4	0	0.7		0	50		39	11	1.3
	Acell	5.3	0.8	2.8		0	63		37	0	1.7
	OS-W	4.3	4.5	0.1		0	39		58	3	0.7
	OS-P	0.1	1.8	1.1		9.4	53		47	0	1.2
	OS-S	0	3.3	0.2		0	0		100	0	0

[a]Expressed as a number per 100 aromatic units (S + G). [b]Molar percentage (S + G + H = 100). [c]From Green Chem. 18:2651, 2016.[11] Indulin AT: softwood kraft, Protobind 1000: mixed straw/grass soda, OS: organosolv wheat straw (OS-W), poplar (OS-P) and spruce (OS-S).

of the HSQC spectra of MWL and selected AHLs are shown in Figure 4 (assignments of main lignin correlation peaks in Table S4).[41−43] The relative percentages of the substructures, such as β-aryl-ether or β-O-4 (A, A′, A″), phenylcoumaran or β-5 (B), resinol or $\beta-\beta$ (C), *p*-hydroxybenzoate substructures (PB), guaiacyl (G or G′), and syringyl (S or S′) were calculated by integrating the contour volumes of the corresponding correlations in the HSQC spectra, as listed in Table 2. Under the mild fractionation severity of P1.5T80t60, the ether side chains were well preserved. The β-O-4 linkage was 54.4%, or retained 94% as compared to MWL (57.8%) (Table 2). At an elevated fractionation severity (P2.5T98t40), the AHL yield was exceptionally good at 81.9% (Table 1) with β-O-4 linkages of 46.2% (Table 2), or the AHL retained approximately 80% ether side chains with respect to MWL.

As has been discussed by others,[24] the success of lignin depolymerization to produce uncondensed lignin relies on the competition between ether cleavage and condensation; preventing the lignin moieties after ether cleavage from direct contact can block or reduce condensation. The rapidity of lignin solubilization by *p*-TsOH in micellular-like aggregates may provide such a hindrance to aldol condensation of β-O-4 cleavage products[44,45] to inert C−C linkages while facilitating fast dissolution and subsequent separation into a solid state at neutral pH. The objective is to produce a lignin sufficiently depolymerized and uncondensed as to be amenable to further processing. The P2.5T98t40 AHL had elevated $S_{condensed}$ (7.2%) and HK (1.9%), as compared to P1.5T80t60 AHL (1.8% and 0.06%, respectively), but both were significantly lower than AHL from the aging or batch process (Table 2) and amenable to Ru/C catalytic depolymerization (discussed later).

To investigate the effect of *p*-TsOH contact time and fractionation temperature on ether linkage condensation, the spent liquor from P2.5T98t40 was aged at different temperatures for various periods of time. Aging at room temperature 20 °C for 72 h (Table 2) resulted in 46% further loss of β-O-4 linkages, a tripling of $S_{condensed}$, and more than 50% loss of signal from G, due to signal loss from condensation. When the same spent liquor was aged at 98 °C for just 30 min, AHL had 63% further loss of β-O-4 linkages, slightly more condensation, and G signal reduction (Figure 4, Table 2). We did, however, demonstrate that immediately cooling the collected spent liquor in an ice bath after collection can reduce AHL darkening due to reduced condensation (Figure S1).

Comparisons with batch fractionation were performed to further elucidate the effects. For example, β-O-4 linkages of AHL from flow-through P3.5T80t60 were comparatively high at 43.9% (76% retention) because of the short contact time between the dissolved AHL with *p*-TsOH. In batch mode under the same set of conditions (P3.5T80t60bat), the majority of the AHL dissolved in the first 30 min (Figure 2C) was essentially aging for the remaining 30 min under *p*-TsOH concentration of 3.5 mol/L and 80 °C, which resulted in substantial AHL condensation and severely reduced β-O-4 linkage to only 4.4% (Figure 4, Table 2). Furthermore, comparisons of the correlations of AHL β-4 linkage content with AHL yield between batch[46] and the present flow-through runs were made (Figure S8A). The results clearly show flow-through substantially expanded the operating window to obtain lignin with a low degree of condensation but at a high yield.

Extended contact of undissolved lignin or lignocellulosic solids with acid can also result in AHL with increased

DOI: 10.1021/acssuschemeng.9b01634
ACS Sustainable Chem. Eng. 2019, 7, 10808−10820

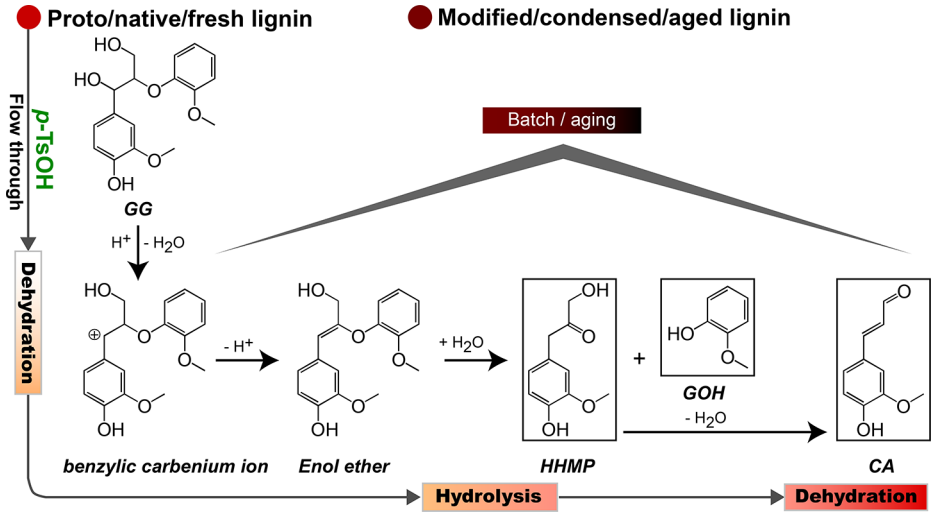

Figure 5. Proposed pathways of acid-catalyzed (*p*-TsOH) lignin depolymerization through *β*-O-4 linkages.

Table 3. Hydroxyl and Carboxyl Group Contents in Lignin Quantified by ^{31}P NMR Using Cholesterol As Internal Standard and Expressed in Millimoles of Functional Groups per Gram of Dry Lignin

	sample labels	aliphatic OH	syringyl OH	condensed guaiacyl OH	guaiacyl OH	*p*-hydroxy phenyl OH	total PhOH	total OH	COOH
extraction	MWL	4.9	0.4	0.08	0.48	0.33	1.3	6.2	0.15
flow-through	P2.5T70t30	3.6	0.6	0.07	0.43	0.48	1.5	5.1	0.08
	P2.5T90t60	2.4	0.6	0.09	0.39	0.37	1.5	3.8	0.12
	P2.5T98t40	3.6	0.8	0.11	0.50	0.46	1.8	5.4	0.06
	P3.6T80t40	3.3	0.7	0.08	0.45	0.42	1.6	4.9	0.09
aging P2.5T98t40	T20t24h	2.4	1.0	0.16	0.53	0.44	2.1	4.5	0.10
	T20t72h	0.6	0.9	0.15	0.34	0.28	1.6	2.3	0.14
	T98t15 min	2.1	1.1	0.17	0.51	0.36	2.1	4.2	0.08
	T98t30 min	2.0	1.5	0.23	0.62	0.35	2.7	4.7	0.10
literature data: Technical and Organosolv Lignin[a]	Indulin Kraft	1.8		1.3[b]	1.3	0.16	2.8	7.3	0.33
	Soda P1000	1.3		1.7	0.73	0.40	2.9	7.0	0.80
	Acell	1.0		1.7	0.58	0.11	3.3	6.7	0.22
	OS-W	1.3		1.2	0.92	0.38	2.5	6.4	0.20
	OS-P	0.8		1.8	0.58	0.18	2.6	6.0	0
	OS-S	1.4		1.2	1.4	0.08	2.7	6.9	0

[a]Data of technical and organosolv lignins were adopted from ref 11. [b]The sum of syringyl OH and condensed guaiacyl OH is equal to 5-substituted phenolic OH in the work of Constant et al., who did not differentiate between syringyl OH and condensed guaiacyl OH.

condensation and reduced *β*-O-4 linkages, as seen by comparing HSQC spectra of AHL from P4.5T70t30 collected at two different periods of time (Figure 4), 0−10 min and 20−30 min. The AHL from 0−10 min was from the fresh raw poplar wood, whereas the AHL from 20−30 min was from the poplar wood that had been soaked in *p*-TsOH solution for 20 min. The AHL from 20−30 min had 17% few *β*-O-4 linkages, a 61% increase in $S_{condensed}$, and a 58% decrease in the G signal as compared to the 0−10 min AHL (Table 2). Although it is recognized that the source lignin of AHL from 0−10 min is not the same as from 20−30 min, the effect of acid contact time with undissolved lignin is nonetheless real.

Despite the presence of condensation products in AHLs, the advantages of low-temperature (below boiling point of water) and rapid *p*-TsOH fractionation can be demonstrated by comparing AHL with lignin from traditional wood delignification technologies that often are carried out at high temperatures (~150 °C) for extended period of time (60−120 min). As shown in Table 2 and Figure S8A, all commercial lignins, such as kraft and organosolv lignin, have less than 10% *β*-O-4 linkages and are highly condensed.

To better understand the structural properties of AHL, *β*-O-4 linked dimeric lignin guaiacylglycerol-*β*-guaiacyl ether (GG) was treated in 2.5 M *p*-TsOH at 90 °C (description for Figure S7). Reaction pathways are summarized in Figure 5. In acidic conditions, a benzylic carbenium ion intermediate is formed by protonation of the *α*-OH in the presence of *p*-TsOH as a strong Brønsted acid. The carbenium ion intermediate is transformed into an enol ether structure after eliminating the *β*-proton.[47] The enol ether is reactive in acidic conditions and is readily hydrolyzed, leading to cleavage of *β*-O-4 ether bond and the formation of 1-hydroxy-3-(4-hydroxy-3-methoxyphenyl)-2- propanone (HHMP) and guaiacol (GOH). HHMP is one of the HKs that were identified in 2D NMR spectra (Figure 4) as discussed earlier. Further dehydration of HHMP led to the formation of coniferyl aldehyde.[29] GC-MS identified products of GOH, HHMP, and coniferyl aldehyde (Figure S9)

DOI: 10.1021/acssuschemeng.9b01634
ACS Sustainable Chem. Eng. 2019, 7, 10808−10820

Table 4. Comparisons of Yields from Reductive Catalytic Depolymerization of AHL, MWL, and Raw Poplar

sample	lignin yield (%)	solid products yield (%)	bio-oil yield (%)	lignin monomer yield (%)	Mn	Mw	PI
$AHL_{P2.5T90t60}$	79	22.9	73	30	29	79	2.7
MWL	low	31.6	64	31	26	46	1.8
untreated poplar	83	51.9	34	41[a]	19	34	1.8

[a]Based on Klason lignin in poplar.

are consistent with the proposed pathway from previous studies.[6,22,48,49]

Semiquantification of HK was conducted to give relative abundance as listed in Table 2. The inverse linear correlation between HK and β-O-4 content (Figure S8B) was consistent with aryl-ether bond cleavage and subsequent formation of HK through benzylic carbenium ion and enol ether intermediates. Hibbert's ketones are reactive in acidic system and tend to repolymerize to form complex condensed structures,[50] especially at harsh treatment conditions, and the inverse correlation between $S_{condensed}$ and β-O-4 is also plotted (Figure S8B).

AHL Functional Groups by ^{31}P NMR. ^{31}P NMR was used to quantify aliphatic OH, syringyl OH, guaiacyl OH, condensed guaiacyl OH, *p*-hydroxy OH, and carboxylic acid groups present in lignin after phosphitylation (Table S5). Hydroxyl groups determined from the ^{31}P NMR spectra (Figure S9) are expressed in mmoles of functional groups per gram of AHL as determined from ^{31}P NMR spectra (Table 3). All AHLs had a lower aliphatic OH content than MWL as a result of dehydration reaction, as illustrated by the reaction pathways (Figure 5). However, AHLs resulting from *p*-TsOH fractionations with a short residence time such as P40T98t40 and P40T70t30 preserved 73.5% aliphatic OH due to reduced dehydration with shortened fractionation times.

All AHLs had a higher phenolic OH content than MWL as a result of cleavage of aryl-ether bonds (Figure 5), especially for those AHLs from high-temperature fractionation or spent liquor aging, such as P2.5T98t40 and P2.5T98t40-AgedT98t30 min (Table 3). The higher phenolic OH appears from the increase in syringyl OH and condensed guaiacyl OH, while free guaiacyl OH and *p*-hydroxy OH were relatively constant.

All AHLs also have a lower COOH content than MWL, similar to Organosolv lignins (Table 3). Kraft and soda lignin from alkaline pulping have high COOH. In summary, AHL has a higher aliphatic OH and a lower phenolic OH than kraft and soda lignin, similar to the levels of MWL, suggesting a comparatively better-preserved chemical structure.

Lignin Aromatics from AHL through Ru/C Depolymerization. To demonstrate the utility of AHL for valorization through further depolymerization to lignin aromatics, we carried out reductive catalytic depolymerization of AHL from P2.5T90t60, MWL, and poplar wood using commercial Ru/C as catalyst in the presence of H_2 with methanol.[12] Reductive depolymerization of AHL resulted in a higher lignin bio-oil yield of 73%, as compared to 64% from MWL, with approximately the same yields of lignin monomers of 30% (Table 4). Given that the $AHL_{P2.5T90t60}$ yield was 79.3% (Table 1), as compared to an MWL yield of less than 20%, it strongly suggests that $AHL_{P2.5T90t60}$ performed better despite β-O-4 content of only 36.1% (Table 2), substantially lower than 57.8% for MWL. This demonstrates that near 100% preservation of β-O-4 linkages is not necessary to achieve excellent lignin monomer yield using reductive depolymerization on the isolated lignin, but suggests that minimizing condensation of the cleaved β-O-4 moieties is key.

Using untreated poplar resulted in a much lower lignin bio-oil yield of 34.1% because the Klason lignin content of poplar was only 23.8% (Table 1) but with a higher lignin monomer yield of 41% than 30% from $AHL_{P2.5T90t60}$, suggesting that AHL has more condensed structures than native lignin in poplar. GPC analyses showed that all three lignin bio-oils had two major peaks at approximately 187 and 417 g/mol (Figure 6A),

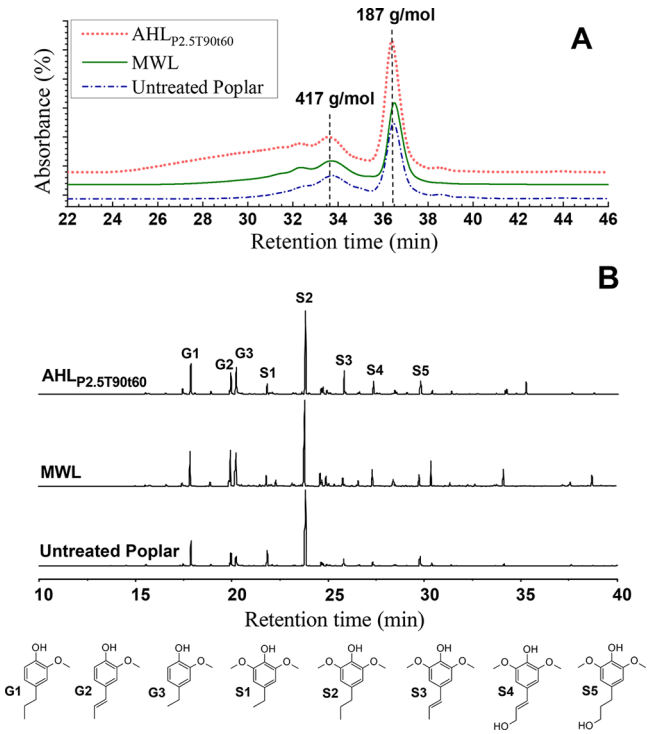

Figure 6. Comparisons of chromatographic analyses of bio-oils from reduction depolymerization of AHL, MWL, and untreated poplar. (A) GPC; (B) GC-MS.

representing lignin monomer and dimers, respectively. The chromatograms of the three lignin bio-oils were very similar. Additional minor peaks can be seen from the chromatograms of bio-oils from $AHL_{P2.5T90t60}$ and MWL. However, the bio-oils derived from the untreated poplar showed almost no minor peaks. The bio-oil from $AHL_{P2.5T90t60}$ also had the broadest molecular weight distribution (Figure 6A), mainly in the high molecular range, and therefore the highest polydispersity index (PI) (Table 4).

GC-MS analyses further validated the GPC analytical results. Overall, the compositions of the three bio-oils were similar (Figure 6B). The main components identified were guaiacol (G1-G2), guaiacyl ethane (G3), and syringyl (S1−S5) lignin subunits. These results indicated that $AHL_{P2.5T90t60}$ with a yield of approximately 80% from fractionation of poplar was highly

DOI: 10.1021/acssuschemeng.9b01634
ACS Sustainable Chem. Eng. 2019, 7, 10808−10820

reactive in reductive catalytic depolymerization with a similar lignin monomer yield as that from MWL.

AHL Physical Properties. Physical properties such as molecular weight (Mw) and glass transition temperature (T_g) are important to direct valorization of AHL as polymers. A low molecular weight may be good for further depolymerization to aromatics through catalysis, as discussed above. A high molecular weight, however, is preferred for direct applications as lignin polymers in composite materials, dispersants, and other products. Molecular weight of solubilized lignin depends not only on the plant species but also on the solubilization process used. Because lignin in wood is heterogeneous and wood has a hierarchical structure, lignin solubilized at different stages of a fractionation process has different physical properties. This can be seen from the time-dependent measurements of AHL molecular weights shown in Figure 7A. The AHL obtained in the first 5 min of flow-through fractionation (0−5 min) under P3.5T80, i.e., relatively high acid concentration and temperature or severity, has a very broad molecular weight distribution with a very large PI of 7.3

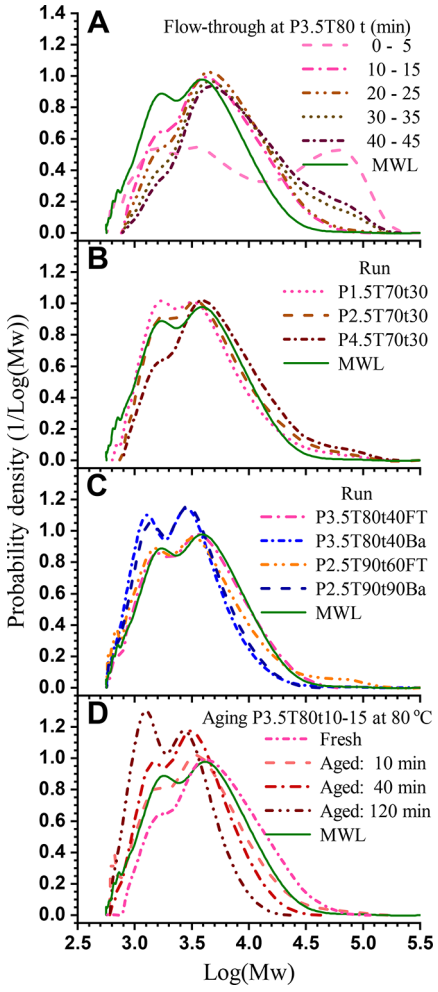

Figure 7. GPC measured molecular weight distributions of AHLs in comparison with that of MWL. (A) AHLs from periodic sampling of process liquor under P3.5T80; (B) AHLs from different *p*-TsOH concentrations at 70 °C for 30 min; (C) AHLs from flow-through vs batch fractionations under two sets of conditions; (D) AHLs from aging spent liquor collected between 15−20 min under P3.5T80 at 80 °C for different times.

(Table 5). It contains low-molecular-weight oligomers (Mw < 1000 Da) as well as very high molecular weight polymers (Mw > 100 000) that represents nearly non-depolymerized native lignin with an average molecular weight (Mw) reaching 19 160 Da (Table 5). The first 5 min fractionation, though a short period time, produced 25.7% (based on Figure 2C) of the total AHL from the entire 40 min fractionation with a yield of 75% (Table 1), or solubilized 19% of wood lignin, a very substantial amount. The amount of very high molecular weight lignin disappeared rapidly with fractionation time (comparing AHL from 0−5 min to 10−15 min, Table 4), demonstrating that the majority of the unsolubilized lignin remaining in the wood was certainly depolymerized through the cleavage of ether bonds in the first 10 min *p*-TsOH fractionation. As a result, both Mw and PI of the AHL from 10−15 min were substantially reduced (Table 5). This again confirms that chemical cleavage did take place in lignin solubilization by *p*-TsOH in addition to physical aggregation. The molecular weight distribution shifted toward the right as fractionation progressed with time due to the release of relatively large molecules and repolymerization (condensation) as discussed early, both of which increase Mw (Table 5). This is further evidenced by the fact that the two AHLs collected from 30−35 min and 40−45 min, with similar molecular weight distributions, had higher probabilities in the high molecular weight tale, higher Mw and Mn (Table 5), than AHLs collected from 10−15 min and 20−25 min. However, the amounts of AHL yield from 30−35 min and 40−45 min were insignificant, as shown in Figure 2C.

Under low fractionation severities, such as under *p*-TsOH concentration below 2.5 mol/L at 70 °C for 30 min, AHL yields were low of less than 25% (Table 1); i.e., the majority of

Table 5. List of GPC Measured Molecular Weights and Glass Transition Temperature (T_g) of AHLs from Various Fractionation Conditions along with Those of MWL

	sample labels	Mw	Mn	PI	T_g (°C)
extraction	MWL	**4094**	**2084**	**1.96**	**137**
flow-through: time-dependent: P3.5T80	P3.5T80t0-5	19160	2620	7.31	
	P3.5T80t10-15	5961	2419	2.46	
	P3.5T80t20-25	6691	2701	2.48	
	P3.5T80t30-35	9729	2937	3.31	
	P3.5T80t40-45	11498	3152	3.65	
flow-through	P1.5T80t90				151
	P2.5T90t60				165
flow-through: acid concentration effect	P1.5T70t30	4740	2092	2.27	
	P2.5T70t30	5741	2179	2.63	
	P4.5T70t30	6807	2243	3.03	
batch vs flow-through	P3.5T80t40	4414	2073	2.13	
	P3.5T80t40bat	2698	1697	1.59	
	P2.5T90t60	4513	1929	2.34	165
	P2.5T90t90bat	3001	1794	1.67	176
	no aging	5961	2419	2.46	
spent liquor aging: P3.5T80t10-15	aged: T80t10 min	5847	2461	2.38	
	aged: T80t40 min	3356	1940	1.73	
	aged: T80t120 min	2759	1784	1.56	

DOI: 10.1021/acssuschemeng.9b01634
ACS Sustainable Chem. Eng. 2019, 7, 10808−10820

wood lignin was not solubilized, just like MWL extraction, to result in similar molecular weight distribution profiles as MWL, as shown in Figure 7B. Increasing *p*-TsOH concentration to 4.5 mol/L, i.e., increasing severity, increased lignin yield to 55% (Table 1) and resulted in a slight shift of the distribution profile toward the large molecular weight region and increased Mw and PI (Table 5) due to the release of large lignin molecules as well as to repolymerization (condensation, Table 2). Under severe fractionation conditions, a batch fractionation has a long contact time between AHL and *p*-TsOH as compared to a flow-through fractionation under the same condition. As a result, AHL molecular weight distribution profile shifted toward the low-molecular-weight region due to substantial lignin depolymerization and cleavage of ether bonds despite repolymerization, as shown in Figure 7C, which reduced Mw, Mn, and PI (Table 5). This is further evidenced by the data from the spent liquor aging study. The left shift toward low molecular weight is pronounced with extended aging time, as shown in Figure 7D. Mw, Mn, and PI were decreased with aging time (Table 5). The reduction in PI is a clear indication of the formation of low-molecular-weight molecules through depolymerization. This is in contrast to increased PI due to increase in acid concentration (severity) under low fractionation severities (T70 for 30 min) without substantial depolymerization discussed above (Table 5). The results in Figure 7 and Table 5 suggest that a moderate fractionation severity can result in AHL with a relatively large Mw by releasing large molecules while preventing substantial lignin depolymerization.

In general, lignin condensation resulted in increased glass transition temperature T_g. As listed in Table 5, the T_g of AHL is increased with fractionation severity or degree of condensation (Table 2), in agreement with our early study in batch mode.[46] The formation of thermostable carbon−carbon bonds by the repolymerization reactions resulted in an elevated T_g, which is unfavorable for certain composite applications.[51]

Future Development. Several important steps needs to be taken to move the AHF process to commercialization, though we do not see regulatory issues as *p*-TsOH is an industry catalyst and widely used in many industries. High value utilization of the cellulosic fraction is certainly the first step. Producing lignin containing cellulose nanomaterials (LCNM) is the best outlet when the commercial market for LCNM is fully developed. This is because minimal delignification (approximately 50%) is needed, which translates to low acid dosage to ease chemical recovery for producing hydrophobic LCNM as demonstrated previously.[27,28] With the developed AHF reaction severity factor as a scale-up factor,[28] no major technical or engineering issues will be encountered. Under a high delignification scenario, the cellulosic fraction is best suited for producing dissolving pulp fibers for textile as most hemicelluloses are removed by AHF. However, bleaching and dissolution of the bleached fibers, as well as the properties of the dissolved materials, need to be evaluated using existing technologies. The second issue that needs to be addressed is chemical recovery. An initial laboratory study indicated that over 95% of the acid remaining on unwashed solids can be recovered.[46] However, full evaluation of acid recovery through evaporation of the diluted (including cellulosic solids washing filtrates) needs to be carried out. In addition to a preliminary batch dehydration study,[28] furfural production needs to be optimized depending on the degree of delignification or xylan dissolution using existing knowledge.[52,53] Lignin separation from *p*-TsOH other than dilution, such as absorption of *p*-TsOH,[54] needs to be evaluated. In addition to the depolymerization evaluation presented in the present work, valorization of AHL for various products needs to be carried out. Finally, all these studies need to be carried out at the pilot scale to obtain meaningful data for techno-economic analyses.

CONCLUSIONS

Acid hydrotyropes such as *p*-TsOH in aqueous systems can rapidly fractionate wood lignin with low degrees of condensation at high yield up to 80% using a flow-through reaction under atmospheric pressure below the boiling point of water. The resultant AHLs with a high content of β-O-4 linkages and high molecular weight of greater than 4500 Da are suitable for direct applications as polymers in composites, as well as subsequent depolymerization to aromatics. Upon reductive catalytic depolymerization, similar yields of lignin monomer of approximately 30% were obtained from an AHL (yield of 80%) as compared to MWL (low yield of ∼20%). AHL also has a pinkish color, suitable for direct applications as dye dispersants, cosmetics, and other products. Acid hydrotrope *p*-TsOH also selectively dissolves hemicelluloses that can be dehydrated into furfural using the *p*-TsOH in the spent liquor without an additional catalyst. The simplicity of using one industrial and recyclable chemical, *p*-TsOH, to valorize all major components of wood at low temperatures in short time frames can be advantageous over existing technologies.

ASSOCIATED CONTENT

Supporting Information

The Supporting Information is available free of charge on the ACS Publications website at DOI: 10.1021/acssuschemeng.9b01634.

Figure S1: Flow-through reactor system for *p*-TsOH fractionation of lignocelluloses at 40 g scale. Figure S2: Images and optical extinctions coefficients of untreated poplar wood, *p*-TsOH treated WISs, MWL, AHL, and KL. Figure S3: Comparisons of xylan recovery between fractionations using *p*-TsOH and GVL. Figure S4: Correlations of experimentally measured lignin and glucan dissolution with xylan dissolution. Figure S5: Correlations between xylose concentrations and acetic acid concentrations measured from periodic sampling of process liquor under three fractionation severities. Figure S6: Effect of process liquor from P2.5T98t40 aging on AHL optical properties. Figure S7: Color development profile of acidolysis reaction products of guaiacylglycerol-beta- guaiacyl ether (GG) in 2.5 M *p*-TsOH at 90 °C over time. Identified reaction products of 1-hydroxy-3-(4-hydroxy-3-methoxyphenyl)-2-propanone (HHMP) and coniferyl aldehyde (CA) from guaiacylglycerol-beta-guaiacyl ether (GG) in 2.5 mol/L *p*-TsOH at 90 °C for 50 min. Figure S8: A: Comparisons of the extent of delignification versus total ether bonds of dissolved lignin among *p*-TsOH fractionation, MWL, and conventional technical and organosolv lignins. B: Correlations between HK and $S_{condensed}$ with β-O-4. Figure S9: Mass spectra of TMS derivatives of guaiacol (GOH), 3-(4-hydroxy-3-methoxyphenyl) propionic acid, and coniferyl aldehyde (CA) from acidolysis experiment of guaiacylglycerol-β-guaiacyl

DOI: 10.1021/acssuschemeng.9b01634
ACS Sustainable Chem. Eng. 2019, 7, 10808−10820

ether (GG) in 2.5 M *p*-TsOH at 90 °C for 50 min. Figure S10: ^{31}P NMR spectra of phosphitylated lignin samples for quantitative determination of functional groups. Table S1: Conditions of flow-through aqueous *p*-TsOH treatments for poplar wood fractionation. Table S2: pH profile of filtrates from washing fractionated lignocellulosic solids in the flow-through reactor. Table S3: Conditions of aging treatments of effluents from flow-through fractionation of poplar wood. Table S4: Assignments of the lignin ^{13}C−^{1}H correlation peaks in the 2D HSQC spectra of milled wood lignin of poplar wood and the isolated AHL. Table S5: Integration regions used for ^{31}P NMR analysis of TMDP phosphitylated lignin (PDF)

AUTHOR INFORMATION

Corresponding Author

*E-mail: junyong.zhu@usda.gov; junyong.zhu@wisc.edu.

ORCID

Shi Qiu: 0000-0002-9522-2292
Jinlan Cheng: 0000-0001-8462-6606
Yunming Fang: 0000-0001-9586-5581
Xuejun Pan: 0000-0002-6859-9342
J.Y. Zhu: 0000-0002-5136-0845

Notes

The authors declare the following competing financial interest(s): J.Y.Z. is a co-inventor of the p-TsOH fractionation process.

ACKNOWLEDGMENTS

This work is partially supported by U.S. Forest Service, the Natural Science Foundation of China (No. 31570571), and Shandong Provincial Education Department (China) which made the visiting appointments of Z.W. and J.C. at the USDA Forest Products Lab (FPL) possible. We also would like to acknowledge Roland Gleisner (FPL) for hammer milling the poplar wood, Fred Matt (FPL) for conducting chemical composition analyses, Doreen Mann (FPL) for Soxhlet extraction, Sally Ralph and Richard Reiner for helping produce MWL, Qilian Ma and Huihui Wang, visiting students from South China University of Technology, for conducting thermogravimetric and differential thermocalorimetric scanning analyses.

REFERENCES

(1) Pan, X.; Gilkes, N.; Kadla, J.; Pye, K.; Saka, S.; Gregg, D.; Ehara, K.; Xie, D.; Lam, D.; Saddler, J. Bioconversion of hybrid poplar to ethanol and co-products using an organosolv fractionation process: Optimization of process yields. *Biotechnol. Bioeng.* **2006**, *94* (5), 851−861.

(2) Zhu, J. Y.; Pan, X. J.; Wang, G. S.; Gleisner, R. Sulfite pretreatment (SPORL) for robust enzymatic saccharification of spruce and red pine. *Bioresour. Technol.* **2009**, *100* (8), 2411−2418.

(3) Iakovlev, M.; van Heiningen, A. Efficient fractionation of spruce by SO2-ethanol-water treatment: Closed mass balances for carbohydrates and sulfur. *ChemSusChem* **2012**, *5* (8), 1625−1637.

(4) Gu, F.; Gilles, W.; Gleisner, R.; Zhu, J. Y. Fermentative high titer ethanol production from a Douglas-fir forest residue without detoxification using SPORL: High SO2 loading at a low temperature. *Ind. Biotechnol.* **2016**, *12* (3), 168−175.

(5) Ewanick, S. M.; Bura, R.; Saddler, J. N. Acid-catalyzed steam pretreatment of lodgepole pine and subsequent enzymatic hydrolysis and fermentation to ethanol. *Biotechnol. Bioeng.* **2007**, *98* (1), 737−746.

(6) Shuai, L.; Amiri, M. T.; Questell-Santiago, Y. M.; Heroguel, F.; Li, Y.; Kim, H.; Meilan, R.; Chapple, C.; Ralph, J.; Luterbacher, J. S. Formaldehyde stabilization facilitates lignin monomer production during biomass depolymerization. *Science* **2016**, *354* (6310), 329−333.

(7) Kringstad, K. P.; Morck, R. ^{13}C NMR Spectra of Kraft Lignins. *Holzforschung* **1983**, *37* (5), 237−244.

(8) Gellerstedt, G.; Lindfors, E. L. Structural changes in lignin during kraft pulping. *Holzforschung* **1984**, *38* (3), 151−158.

(9) Rinaldi, R.; Jastrzebski, R.; Clough, M. T.; Ralph, J.; Kennema, M.; Bruijnincx, P. C. A.; Weckhuysen, B. M. Paving the Way for Lignin Valorisation: Recent Advances in Bioengineering, Biorefining and Catalysis. *Angew. Chem., Int. Ed.* **2016**, *55* (29), 8164−8215.

(10) Deuss, P. J.; Lancefield, C. S.; Narani, A.; De Vries, J. G.; Westwood, N. J.; Barta, K. Phenolic acetals from lignins of varying compositions: Via iron(iii) triflate catalysed depolymerisation. *Green Chem.* **2017**, *19* (12), 2774−2782.

(11) Constant, S.; Wienk, H. L. J.; Frissen, A. E.; Peinder, P. D.; Boelens, R.; Van Es, D. S.; Grisel, R. J. H.; Weckhuysen, B. M.; Huijgen, W. J. J.; Gosselink, R. J. A.; Bruijnincx, P. C. A. New insights into the structure and composition of technical lignins: A comparative characterisation study. *Green Chem.* **2016**, *18* (9), 2651−2665.

(12) Van Den Bosch, S.; Schutyser, W.; Vanholme, R.; Driessen, T.; Koelewijn, S. F.; Renders, T.; De Meester, B.; Huijgen, W. J. J.; Dehaen, W.; Courtin, C. M.; Lagrain, B.; Boerjan, W.; Sels, B. F. Reductive lignocellulose fractionation into soluble lignin-derived phenolic monomers and dimers and processable carbohydrate pulps. *Energy Environ. Sci.* **2015**, *8* (6), 1748−1763.

(13) Galkin, M. V.; Samec, J. S. M. Lignin Valorization through Catalytic Lignocellulose Fractionation: A Fundamental Platform for the Future Biorefinery. *ChemSusChem* **2016**, *9* (13), 1544−1558.

(14) Sun, Z.; Fridrich, B.; De Santi, A.; Elangovan, S.; Barta, K. Bright Side of Lignin Depolymerization: Toward New Platform Chemicals. *Chem. Rev.* **2018**, *118* (2), 614−678.

(15) Wang, S.; Shuai, L.; Saha, B.; Vlachos, D. G.; Epps, T. H. From Tree to Tape: Direct Synthesis of Pressure Sensitive Adhesives from Depolymerized Raw Lignocellulosic Biomass. *ACS Cent. Sci.* **2018**, *4* (6), 701−708.

(16) Ferrini, P.; Rinaldi, R. Catalytic biorefining of plant biomass to non-pyrolytic lignin bio-oil and carbohydrates through hydrogen transfer reactions. *Angew. Chem., Int. Ed.* **2014**, *53* (33), 8634−8639.

(17) Parsell, T.; Yohe, S.; Degenstein, J.; Jarrell, T.; Klein, I.; Gencer, E.; Hewetson, B.; Hurt, M.; Kim, J. I.; Choudhari, H.; Saha, B.; Meilan, R.; Mosier, N.; Ribeiro, F.; Delgass, W. N.; Chapple, C.; Kenttamaa, H. I.; Agrawal, R.; Abu-Omar, M. M. A synergistic biorefinery based on catalytic conversion of lignin prior to cellulose starting from lignocellulosic biomass. *Green Chem.* **2015**, *17* (3), 1492−1499.

(18) Anderson, E. M.; Katahira, R.; Reed, M.; Resch, M. G.; Karp, E. M.; Beckham, G. T.; Roman-Leshkov, Y. Reductive Catalytic Fractionation of Corn Stover Lignin. *ACS Sustainable Chem. Eng.* **2016**, *4* (12), 6940−6950.

(19) Kumaniaev, I.; Subbotina, E.; Savmarker, J.; Larhed, M.; Galkin, M. V.; Samec, J. S. M. Lignin depolymerization to monophenolic compounds in a flow-through system. *Green Chem.* **2017**, *19* (24), 5767−5771.

(20) Galkin, M. V.; Smit, A. T.; Subbotina, E.; Artemenko, K. A.; Bergquist, J.; Huijgen, W. J. J.; Samec, J. S. M. Hydrogen-free catalytic fractionation of woody biomass. *ChemSusChem* **2016**, *9* (23), 3280−3287.

(21) Sun, Z.; Bottari, G.; Afanasenko, A.; Stuart, M. C. A.; Deuss, P. J.; Fridrich, B.; Barta, K. Complete lignocellulose conversion with integrated catalyst recycling yielding valuable aromatics and fuels. *Nature Catalysis* **2018**, *1* (1), 82−92.

(22) Schutyser, W.; Renders, T.; Van Den Bosch, S.; Koelewijn, S. F.; Beckham, G. T.; Sels, B. F. Chemicals from lignin: An interplay of

DOI: 10.1021/acssuschemeng.9b01634
ACS Sustainable Chem. Eng. 2019, 7, 10808−10820

lignocellulose fractionation, depolymerisation, and upgrading. *Chem. Soc. Rev.* **2018**, *47* (3), 852−908.
(23) Li, N.; Li, Y.; Yoo, C. G.; Yang, X.; Lin, X.; Ralph, J.; Pan, X. An uncondensed lignin depolymerized in the solid state and isolated from lignocellulosic biomass: A mechanistic study. *Green Chem.* **2018**, *20* (18), 4224−4235.
(24) Alonso, D. M.; Hakim, S. H.; Zhou, S.; Won, W.; Hosseinaei, O.; Tao, J.; Garcia-Negron, V.; Motagamwala, A. H.; Mellmer, M. A.; Huang, H.; Houtman, C. J.; Labbe, N.; Harper, D. P.; Maravelias, C.; Runge, T.; Dumesic, J. A. Increasing the revenue from lignocellulosic biomass: Maximizing feedstock utilization. *Sci. Adv.* **2017**, *3*, e1603301.
(25) Ma, Y.; Hummel, M.; Kontro, I.; Sixta, H. High performance man-made cellulosic fibres from recycled newsprint. *Green Chem.* **2018**, *20* (1), 160−169.
(26) Zhu, J. Y.; Chen, L.; Gleisner, R., Low temperature and efficient fractionation of lignocellulosic biomass using recyclable organic solid acids. *U.S. Patent*, US20180215774A1, 2018.
(27) Bian, H.; Chen, L.; Gleisner, R.; Dai, H.; Zhu, J. Y. Producing wood-based nanomaterials by rapid fractionation of wood at 80 °C using a recyclable acid hydrotrope. *Green Chem.* **2017**, *19*, 3370−3379.
(28) Ma, Q.; Zhu, J.; Gleisner, R.; Yang, R.; Zhu, J. Y. Valorization of wheat straw using a recyclable hydrotrope at low temperatures (≤90 °C). *ACS Sustainable Chem. Eng.* **2018**, *6*, 14480−14489.
(29) Lancefield, C. S.; Panovic, I.; Deuss, P. J.; Barta, K.; Westwood, N. J. Pre-treatment of lignocellulosic feedstocks using biorenewable alcohols: towards complete biomass valorisation. *Green Chem.* **2017**, *19* (1), 202−214.
(30) Rahimi, A.; Ulbrich, A.; Coon, J. J.; Stahl, S. S. Formic-acid-induced depolymerization of oxidized lignin to aromatics. *Nature* **2014**, *515* (7526), 249−252.
(31) Luterbacher, J. S.; Azarpira, A.; Motagamwala, A. H.; Lu, F.; Ralph, J.; Dumesic, J. A. Lignin monomer production integrated into the γ-valerolactone sugar platform. *Energy Environ. Sci.* **2015**, *8* (9), 2657−2663.
(32) Si, X.; Lu, F.; Chen, J.; Lu, R.; Huang, Q.; Jiang, H.; Taarning, E.; Xu, J. A strategy for generating high-quality cellulose and lignin simultaneously from woody biomass. *Green Chem.* **2017**, *19* (20), 4849−4857.
(33) Chen, L.; Dou, J.; Ma, Q.; Li, N.; Wu, R.; Bian, H.; Yelle, D. J.; Vuorinen, T.; Fu, S.; Pan, X.; Zhu, J. Y. Rapid and near-complete dissolution of wood lignin at ≤ 80 °C by a recyclable acid hydrotrope. *Sci. Adv.* **2017**, *3* (9), e1701735.
(34) Luo, X.; Gleisner, R.; Tian, S.; Negron, J.; Horn, E.; Pan, X. J.; Zhu, J. Y.; Zhu, W. Evaluation of mountain beetle infested lodgepole pine for cellulosic ethanol production by SPORL pretreatment. *Ind. Eng. Chem. Res.* **2010**, *49* (17), 8258−8266.
(35) Wen, J.-L.; Yuan, T.-Q.; Sun, S.-L.; Xu, F.; Sun, R.-C. Understanding the chemical transformations of lignin during ionic liquid pretreatment. *Green Chem.* **2014**, *16* (1), 181−190.
(36) Xiao, L. P.; Wang, S.; Li, H.; Li, Z.; Shi, Z. J.; Xiao, L.; Sun, R. C.; Fang, Y.; Song, G. Catalytic Hydrogenolysis of Lignins into Phenolic Compounds over Carbon Nanotube Supported Molybdenum Oxide. *ACS Catal.* **2017**, *7* (11), 7535−7542.
(37) Luterbacher, J. S.; Rand, J. M.; Alonso, D. M.; Han, J.; Youngquist, J. T.; Maravelias, C. T.; Pfleger, B. F.; Dumesic, J. A. Nonenzymatic sugar production from biomass using biomass-derived γ-valerolactone. *Science* **2014**, *343* (6168), 277−280.
(38) Scheller, H. V.; Ulvskov, P. Hemicelluloses. *Annu. Rev. Plant Biol.* **2010**, *61*, 263−289.
(39) Ajao, O.; Jeaidi, J.; Benali, M.; Restrepo, A. M.; El Mehdi, N.; Boumghar, Y. Quantification and variability analysis of lignin optical properties for colour-dependent industrial applications. *Molecules* **2018**, *23* (2), 377.
(40) Higuchi, T.; Ito, T.; Umezawa, T.; Hibino, T.; Shibata, D. Red-brown color of lignified tissues of transgenic plants with antisense CAD gene: Wine-red lignin from coniferyl aldehyde. *J. Biotechnol.* **1994**, *37* (2), 151−158.
(41) Yuan, T.-Q.; Sun, S.-N.; Xu, F.; Sun, R.-C. Characterization of lignin structures and lignin−carbohydrate complex (LCC) linkages by quantitative 13C and 2D HSQC NMR spectroscopy. *J. Agric. Food Chem.* **2011**, *59* (19), 10604−10614.
(42) Del Río, J. C.; Rencoret, J.; Prinsen, P.; Martínez, A. T.; Ralph, J.; Gutierrez, A. Structural characterization of wheat straw lignin as revealed by analytical pyrolysis, 2D-NMR, and reductive cleavage methods. *J. Agric. Food Chem.* **2012**, *60* (23), 5922−5935.
(43) Yelle, D. J.; Ralph, J.; Frihart, C. R. Characterization of nonderivatized plant cell walls using high-resolution solution-state NMR spectroscopy. *Magn. Reson. Chem.* **2008**, *46* (6), 508−517.
(44) Deuss, P.; Scott, M.; Tran, F.; Westwood, N.; de Vries, J.; Barta, K. Aromatic Monomers by in Situ Conversion of Reactive Intermediates in the Acid-Catalyzed Depolymerization of Lignin. *J. Am. Chem. Soc.* **2015**, *137* (23), 7456−7467.
(45) Imai, T.; Yokoyama, T.; Matsumoto, Y. Revisiting the mechanism of β-O-4 bond cleavage during acidolysis of lignin IV: Dependence of acidolysis reaction on the type of acid. *J. Wood Sci.* **2011**, *57* (3), 219−225.
(46) Cheng, J.; Hirth, K.; Ma, Q.; Zhu, J.; Wang, Z.; Zhu, J. Y. Toward sustainable and complete wood valorization by fractionating lignin with low condensation using an acid hydrotrope at low temperatures (≤ 80° C). *Ind. Eng. Chem. Res.* **2019**, *58*, 7063.
(47) Yokoyama, T.; Matsumoto, Y. Revisiting the mechanism of β-O-4 bond cleavage during acidolysis of lignin. Part 1: Kinetics of the formation of enol ether from non-phenolic C6-C2 type model compounds. *Holzforschung* **2008**, *62* (2), 164−168.
(48) Adler, E.; Pepper, J.; Eriksoo, E. Action of mineral acid on lignin and model substances of guaiacylglycerol-β-aryl ether type. *Ind. Eng. Chem.* **1957**, *49* (9), 1391−1392.
(49) Sturgeon, M. R.; Kim, S.; Lawrence, K.; Paton, R. S.; Chmely, S. C.; Nimlos, M.; Foust, T. D.; Beckham, G. T. A Mechanistic Investigation of Acid-Catalyzed Cleavage of Aryl-Ether Linkages: Implications for Lignin Depolymerization in Acidic Environments. *ACS Sustainable Chem. Eng.* **2014**, *2*, 472−485.
(50) Shuai, L.; Amiri, M. T.; Luterbacher, J. S. The influence of interunit carbon−carbon linkages during lignin upgrading. *Curr. Opin. Green Sustainable Chem.* **2016**, *2*, 59−63.
(51) Glasser, W. G.; Loos, R.; Cox, B.; Cao, N. Melt-blown compostable polyester films with lignin. *Tappi J.* **2017**, *16* (3), 111−121.
(52) Mandalika, A.; Runge, T. Enabling integrated biorefineries through high-yield conversion of fractionated pentosans into furfural. *Green Chem.* **2012**, *14* (11), 3175−3184.
(53) Weingarten, R.; Cho, J.; Conner, W. C., Jr.; Huber, G. W. Kinetics of furfural production by dehydration of xylose in a biphasic reactor with microwave heating. *Green Chem.* **2010**, *12* (8), 1423−1429.
(54) Woodward, R. T.; Kessler, M.; Lima, S.; Rinaldi, R. Hypercrosslinked microporous polymer sorbents for the efficient recycling of a soluble acid catalyst in cellulose hydrolysis. *Green Chem.* **2018**, *20* (10), 2374−2381.

DOI: 10.1021/acssuschemeng.9b01634
ACS Sustainable Chem. Eng. 2019, 7, 10808−10820